American Mineralogist, Volume 110, pages 1677–1685, 2025

On the labyrinthine crystal-chemistry of boleite, a Pb-Ag-Cu hydroxyhalide

G. Diego Gatta[1,*], Giorgio Guastella[2], Pierino Malizia[2], Tommaso Battiston[1], Marco Merlini[1], Geoffrey Bromiley[3], and Oscar Fabelo[4]

[1]Dipartimento di Scienze della Terra, Università degli Studi di Milano, Via Botticelli 23, I-20133 Milano, Italy
[2]Agenzia delle Dogane e dei Monopoli – Direzione territoriale Lombardia – Ufficio Laboratorio di Milano, Via Marco Bruto 14, I-20138 Milano, Italy
[3]School of GeoSciences, The University of Edinburgh, Edinburgh EH8 9XP, U.K.
[4]Institut Laue-Langevin, 71 Avenue des Martyrs, F-38000 Grenoble, France

Abstract

The chemical composition and crystal structure of boleite from the Amelia Mine (Boléo District, Mexico) were investigated by a series of chemical analytical techniques and single-crystal X-ray (data collected at 293 K) and neutron diffraction (at 20 K). The concentrations of more than 60 elements were measured. The empirical formula of boleite, based on the multi-analytical approach, is: $(K_{0.390}Ca_{0.165}Na_{0.095}Rb_{0.075}Cd_{0.040}Cs_{0.035}Tl_{0.002})_{\Sigma 0.80}Pb_{26.05}Ag_{8.93}Cu_{23.91}Cl_{61.64}(OH)_{48.39}$, of which the simplified formula should be given as $(K,Ca,Na,Rb,Cd,Cs)Pb_{26}Ag_9Cu_{24}Cl_{62}(OH)_{48}$. However, as Cd can also be considered as a potential substituent for Ag or Cu, the simplified formula transforms to $(K,Ca,Na,Rb,Cs)Pb_{26}Ag_9Cu_{24}Cl_{62}(OH)_{48}$. This finding indicates a more complex scenario with respect to the previous formula reported in the literature, i.e., $KPb_{26}Ag_9Cu_{24}Cl_{62}(OH)_{48}$. Chemical data obtained in this study show no significant evidence of potential substituents of Pb, Ag, and Cu; the concentrations of REE, PGE, and other industrially relevant elements are insignificant. Despite a lack of crystallographic evidence, chemical data appear to suggest that partial Cl^- vs. OH^- substitution can occur. Other potential substituents of Cl^-, such as F^-, have not been detected at a significant level. X-ray and neutron diffraction data confirm the previously reported general structural model of boleite but consistently show that a substitutional disorder affects the *K* site, manifested by a large and unusual displacement parameter. The magnitude of the displacement parameter reflects static disorder, in the form of substitutional disorder, due to differences in the local bonding topology among K, Ca, Na, Rb, (Cd), and Cs statistically populating the same site. The H-bonding network in the structure of boleite is now unambiguously described on the basis of the neutron structural model, with two energetically favorable bonds, both having an O_{donor}-H···$Cl_{acceptor}$ configuration. The structure of boleite does not contain H_2O molecules but, instead, only two crystallographically independent hydroxyl groups.

Keywords: Boleite, crystal chemistry, X-ray diffraction, neutron diffraction, hydrogen bonding

Introduction

Boleite is a rare mineral, which usually occurs in nature in the form of Prussian-blue to indigo cubic crystals, up to 1–2 cm in size, infrequently modified by {111} and {011}. Crystals are translucent to opaque, with a Mohs hardness of 3.0–3.5. Epitactic growth of boleite and other related minerals (i.e., pseudoboleite and cumengeite) can produce unusual forms made by the combination of cube+octahedron or tetragonal pyramid+cube. Boleite was discovered at the Boléo District, Santa Rosalía, Mulegé Municipality, Baja California Sur, Mexico, by French mineralogists M.M.E. Mallard and E. Cumenge (1891), who provided the first data pertaining to the morphological crystallography, some physical properties (e.g., density, hardness, refraction index), and the first chemical composition of the mineral based on a series of chemical analyses: Ag 8.50–8.85 wt%, Cu 13.95–15.00 wt%, Pb 48.45–48.90 wt%, Cl 19.00–19.55 wt%, O 3.77–4.05 wt%, H_2O 4.00–4.28 wt%. Boleite was, therefore, considered as a Pb-Ag-Cu oxychloride mineral, with potential chemical formula: 3[PbCl(OH)·CuCl(OH)]+AgCl. Due to its rarity, this mineral was not considered a commodity for Ag, Cu, or Pb. As boleite's intense blue color is very attractive, this mineral has been used as a pigment or as a gemstone (especially in the past), but its low hardness is a limiting factor for the modern gemstones market. After the report of Mallard and Cumenge (1891), only a few studies have been devoted to boleite (e.g., Friedel 1906; Gossner 1928; Hocart-Strasbourg 1930) until the structure solution, based on single-crystal X-ray intensity data, reported by Rouse (1973). Rouse (1973) showed that the structure of boleite is describable with a cubic unit cell (with $a = 15.29$ Å) and in the space group $Pm\bar{3}m$. The chemical formula derived by Rouse (1973), based on the structural refinement, is: $Pb_{26}Ag_9Cu_{24}Cl_{62}(OH)_{48}$. However, this formula is charge-imbalanced, with an excess charge of 1^-. This led to further investigations, which in part increased the confusion on the actual chemical formula of boleite, as that reported by Abdul-Samad et al. (1981), who inferred the presence of an additional H-atom disordered over the unit cell, and provided a revised formula $Pb_{26}Ag_9Cu_{24}Cl_{62}(OH)_{47}(H_2O)$, or that reported in the Powder Diffraction File (ref. number PDF 72-1529) listing $Pb_{26}Ag_{10}Cu_{24}Cl_{62}(OH)_{48}·3H_2O$. The scenario becomes clearer

* Corresponding author E-mail: diego.gatta@unimi.it Orcid https://orcid.org/0000-0001-8348-7181

0003-004X/25/0010–1677$05.00/DOI: https://doi.org/10.2138/am-2024-9721

only with the study of Cooper and Hawthorne (2000), who reinvestigated the crystal chemistry of boleite by single-crystal X-ray diffraction, electron-microprobe analysis in wavelength-dispersive mode, and infrared spectroscopy. The structural model of Cooper and Hawthorne (2000) confirmed the general findings of Rouse (1973):

- The structure of boleite contains complex chains made by cages linked along the principal crystallographic directions (Figs. 1a–1b).
- One chain system is made by cages consisting of six $AgCl_5$ groups that form square pyramids [whose square faces describe a cube centered at (0,0,0)] connected by $AgCl_6$-octahedra and running along [001], [100], and [010] (Fig. 1a); and
- An additional chain system consists of large cages made by the interconnection of [6Pb+12Cl] sites (with 18 nodes) connected by smaller [6Pb+8Cl] cages (with 14 nodes) and running along [001], [100], and [010] (Fig. 1b).
- At the center of the large 18-node cage, a crystallographic site, occupied by K, lies at ½, ½, ½ (Figs. 1b–1d).
- Two crystallographically independent OH-groups occur.
- The structure does not contain H_2O molecules (as verified by IR data).

Based on their chemical and crystallographic findings, Cooper and Hawthorne (2000) revised the ideal formula of boleite to $KPb_{26}Ag_9Cu_{24}Cl_{62}(OH)_{48}$, which is charge balanced. The absence of molecular H_2O in the structure of boleite was later confirmed by Frost et al. (2003) and Frost and Williams (2004), by Raman spectroscopy: the Raman spectrum provided evidence of stretching and deformation modes ascribable only to hydroxyl groups. However, some concerns about the crystal chemistry of boleite remain:

- The weight fraction of K measured by EPMA-WDS (and confirmed later by LA-ICP-MS data), as reported by Cooper and Hawthorne (2000), is only 0.17(2) wt%, whereas the expected amount is 0.36 wt% for 1 K atom per formula unit. Other elements, potentially replacing K as Na, Rb, Cs, Ca, Sr, and Ba, were sought, but below the limits of detection (Cooper and Hawthorne 2000). A full chemical characterization was not performed (or, at least, not reported) by Cooper and Hawthorne (2000). More surprisingly, we did not find any full chemical characterization of boleite reported in the (open) literature during the last 100 years.
- The displacement parameter of the *K* site, refined by X-ray intensity data, is abnormally high, compared to those of the other crystallographic sites (Cooper and Hawthorne 2000). This finding could reflect a static positional disorder promoted by an actual multi-element population in the large [6Pb+12Cl]-cage, with slightly different bonding geometry with the Cl sites.

In this light, the aim of this study is a reinvestigation of the crystal chemistry of a natural boleite (from the Amelia Mine, Boléo District) on the basis of a multi-methodological approach, based on single-crystal X-ray and neutron diffraction, and a series of chemical analytical techniques to: (1) provide a full chemical description of this mineral using modern protocols for major, minor, and trace elements; (2) unveil potential replacement mechanisms at the *K* site not described so far, along with potential substitutions at the Pb-, Cu-, and Ag-sites; and (3) describe unambiguously the location and the anisotropic displacement regime of the proton sites, along with the H-bonding configuration in the structure of boleite, which is expected to have O···Cl (donor-acceptor) interaction.

Sample Description and Occurrence

Some indigo blue crystals of boleite, with cubic habit and edge lengths of about 0.8–1 cm each, from the Amelia Mine, Boléo District, Santa Rosalía, Baja California Sur, Mexico, were used in this study, kindly provided by "Museo delle collezioni mineralogiche, gemmologiche, petrografiche e giacimentologiche" of the University of Milan (ref. #S156).

The Boléo deposit is classified as a "Sediment-hosted Stratiform Copper deposit" (SSC) (Del Rio Salas et al. 2008). It is a low-grade, sediment-hosted, stratiform Cu-Co-Zn deposit, developed in response to early continental rifting with the opening of the Gulf of California. Metal zonation, stratigraphic position, and sedimentary textures and structures support a model of syn-sedimentary ore deposition. As reported by Conly (2003), magmatic fluids likely played an important role in the ore-forming process, as leaching of metals from the underlying volcanic formations, or even from the crystalline basement, cannot account for the total amount of metals in the deposit. Boleite is a secondary mineral, formed through reaction of chloride with primary sulfides in the oxidized zone of the deposit, and coexists with cuprite Cu_2O, carbonates like azurite $Cu_3(CO_3)_2(OH)_2$ and malachite $Cu_2CO_3(OH)_2$, silicates [e.g., chrysocolla $Cu_2H_2Si_2O_5(OH)_4$], atacamite $Cu_2Cl(OH)_3$, cumengeite $Pb_{21}Cu_{20}Cl_{42}(OH)_{40}\cdot 6H_2O$ and pseudoboleite $Pb_{31}Cu_{24}Cl_{62}(OH)_{48}$, along with a series of other minor minerals (Wilson and Rocha 1955). Exceptional crystals, with almost perfect cubic habit (edge length up to 2 cm) and homogeneous Prussian blue to indigo color, are from the Amelia mine of the Boléo District. Additional details about the geology and mineral deposits of the Boléo copper district can be found in Wilson and Rocha (1955).

Experimental Methods and Results

Chemical characterization

The chemical composition of the boleite crystals in this study was first investigated by electron probe microanalysis in wavelength-dispersive mode (EPMA-WDS), with a JEOL 8200 Super Probe system at the COSPECT facility, University of Milan, with the following operating conditions: 15 kV and 5 nA, 5 μm beam diameter, 30 s of counting times on the peaks, and 10 s on the backgrounds. Three millimetric crystal fragments were mounted in epoxy resin (round sample mount 1.0 inch in diameter); the sample surface was polished and then coated with a thin film of electrically conductive carbon. A series of natural and synthetic compounds was used as standards; data were corrected for matrix effects using a ZAF routine implemented in the JEOL suite of programs. The standards employed were: K-feldspar (K), omphacite (Na), pollucite (Cs), $RbMnF_3$ (Rb), metallic Ag (Ag), metallic Cu (Cu), PbO (Pb), forsterite-154 (Mg), fayalite-143 (Fe), grossular (Al, Si, Ca), scapolite (Cl), and apatite (F). The crystal fragments of boleite under investigation were found to be homogeneous. Only K, Ca, Na, Pb, Ag, Cu, and Cl were measured at a significant level;

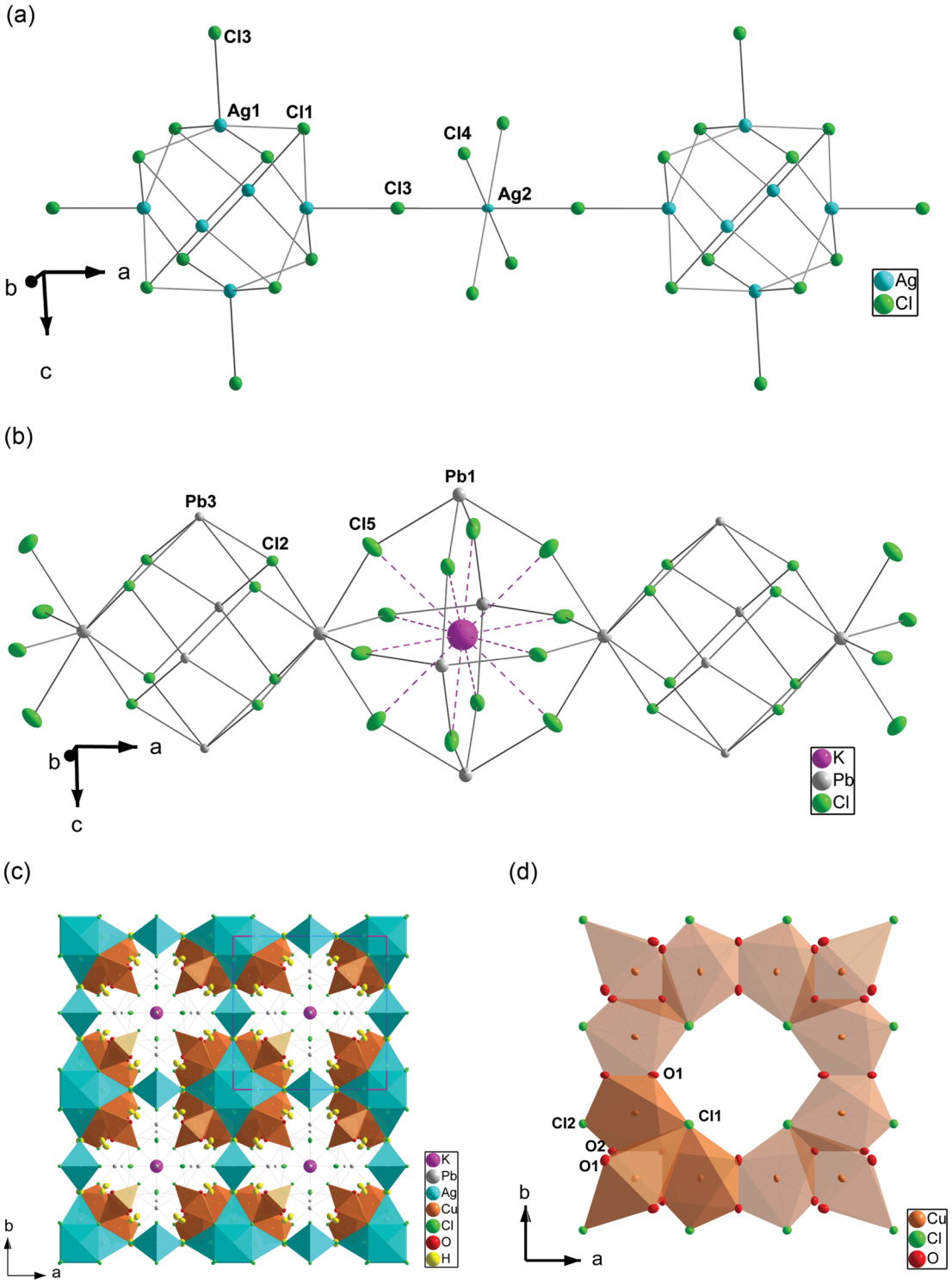

Figure 1. Crystal structure of boleite, based on the neutron structure refinement of this study. (**a**) Chain made by cages consisting of six $AgCl_5$ groups that form square pyramids [whose square faces describe a cube centered at (0,0,0)] connected by $AgCl_6$-octahedra and running along the three principal crystallographic directions; (**b**) chain system consisting of large cages made by the interconnection of [6Pb+12Cl] sites (with 18 nodes), connected by smaller [6Pb+8Cl] cages (with 14 nodes) and running along the three principal crystallographic directions; (**c**) general view of the structure down [001], with Ag- and Cu-polyhedra (see Table 3 for details) and unit cell (top-left); (**d**) clusters made by three face-sharing distorted CuO_4Cl_2 octahedra connected to form 8-membered rings perpendicular to each of the fourfold axes. Displacement ellipsoid probability factor: 90%. (Color online.)

Rb and Cs were not detected. However, degradation of the crystals was observed under the electron beam, even after increasing the beam diameter from 5 to 20 μm, which reduced the quality of the chemical data. After a series of tests, the EPMA-WDS data were considered only at a qualitative level, and a different protocol for quantitative chemical characterization was adopted, based on wet analyses as described below.

Due to the paucity of the sample, a total mass of about 1.1 g of boleite was devoted to chemical characterization of boleite using the following multi-methodological approach. A series of preliminary tests was performed to identify which elements were present at concentrations higher than 0.001 wt%. In this light, a mass of about 600 mg of the sample was used for a preliminary characterization by total carbon-nitrogen-hydrogen (CHN) analysis (on pristine material), total fluorine content by ion-selective electrode (in solution), loss-on-drying (pristine material) and other screening tests performed by wavelength-dispersive X-ray fluorescence (WD-XRF) (pristine material and precipitates), attenuated total reflection in conjunction with infrared spectroscopy (ATR-IR) (pristine material), inductively coupled plasma-mass spectrometry (ICP-MS) and inductively coupled plasma optical emission spectroscopy (ICP-OES) (solutions), and X-ray powder diffraction (PD-XRD) (for precipitates). The only elements found with concentrations higher than 0.001 wt% in the sample of boleite were: Pb, Cl, Cu, Ag, K, Ca, Na, Rb, Cs, Cd, Tl, H (in the form of hydroxyl groups, as shown by ATR-IR) and O. Correspondingly, the remnant mass of about 500 mg of the boleite sample was used for a second round of analyses of the Pb, Ag, Cu, and Cl concentrations by gravimetric methods and titration, and other minor elements concentration by ICP-OES and ICP-MS. The following instruments were employed: WD-XRF-Thermo Scientific ARL Perform'X Sequenzial spectrometer, ATR-IR–Thermo Scientific Nicolet iS10–iTR/iD5 spectrometer, PD-XRD–Bruker D8 Advance diffractometer, perfectION Combination Fluoride Ion Selective Electrode (Mettler Toledo) for the fluorine concentration, Leco CHN Truspec analyzer for the total CHN content, Perkin Elmer Optima 7000DV ICP-OES spectrometer, Thermo Scientific iCAP TQe ICP-MS spectrometer, and a Sartorius ME235P Genius Analytical Balance.

Additional details pertaining to instruments and analytical methods are provided in the following sections. A flow-chart of the complex analytical protocol used in this study is deposited as Online Materials[1] Figure S1.

Gravimetric determination of (insoluble) Ag and Cl

In subdued light, about 500 mg of the sample was placed in a 250 mL beaker, and 100 mL of 2% nitric acid was added. The beaker was covered with a clock glass and heated at a temperature below the boiling point. After 1 h, a white precipitate was collected on a preweighed 30 mL sintered-glass filtering crucible (m_1) (porosity no. 4). The precipitate was washed three times with 10 mL of 5:1000 nitric acid solution and then 3 times with 3 mL of 1:1000 nitric acid solution. The crucible was dried at 130 °C until a constant weight (m_2) was obtained (time: about 4 h). The weight difference (m_2–m_1) represents the total of Ag+Cl insoluble content of the solution, as AgCl. Purity of AgCl was more than 99.95% m/m. The nature of the precipitate was identified by X-ray powder diffraction (chlorargyrite-type), and its purity was determined by ICP-OES and ICP-MS, after dissolution in 10 mL of hydrochloric acid and dilution with water, as described in detail below. The filtrate (clear blue solution, AgCl-free) was transferred to a preweighed 200 mL flask with water. The weight of the final solution was about 200 g. This solution was named "Solution A," and used for measuring the concentration of other elements, excluding C, H, N, and F, as described below. The measured fraction of (insoluble) AgCl in boleite was 11.7(2) wt%.

Determination of (soluble) Cl, Pb and Cu concentration

Gravimetric method for (soluble) Cl concentration and separation from Pb and Cu. About 100 g of the aforementioned "Solution A" was placed in a 200 mL beaker, and 0.1 M silver nitrate solution was added slowly, while constantly stirring, until a slight excess. The suspension was heated nearly to boiling and maintained at this temperature until the coagulation of the precipitate was completed and the supernatant liquid was clear (time: a few minutes). The beaker was then set aside in the dark for 1 h. The precipitate was collected, as described before for the insoluble Ag+Cl. The difference in weight (after drying at 130 °C) reflects the soluble Cl concentration in boleite, obtained as AgCl, measured at 17.1(2) wt%.

The filtrate (clear blue solution) was then named "Solution B" and used for determining Pb and Cu concentrations.

Gravimetric method for Pb concentration and separation from Cu. "Solution B" was placed in a 200 mL beaker, and 0.2 M hydrochloric acid was added slowly until a slight excess. AgCl precipitate was filtered and discarded, as already described, and the filtrate was transferred to a porcelain capsule. Concentrated sulfuric acid (5 mL) was added, and the solution was heated until white fumes of sulfuric acid were generated. After cooling, 50 mL of water was added, and the solution was allowed to settle. After about 4 h, the white precipitate was collected on a preweighed 30 mL porcelain filtering crucible (m_1) (porosity no. 4), washed a few times with 5–10 mL of a washing solution containing 4 mL concentrated sulfuric acid, 100 mL water, and 100 mL ethanol, and then 2–3 times with 5 mL of ethanol. The porcelain crucible was dried at 100 °C for 30 min and then heated to 400 °C in a muffle furnace until a constant weight was achieved (m_2). The difference in weight (m_2–m_1) represents the total Pb content, given as $PbSO_4$. The experimental weight fraction of Pb in boleite was determined to be 49.5(4) wt%.

The filtrate (clear blue solution) was then named "Solution C" and used for measuring the Cu concentration.

Determination of Cu concentration by iodometric titration. The "Solution C" was transferred to a 200 mL beaker and boiled to a final volume of 25 mL. After cooling, ammonium hydroxide was added until a basic pH was measured, and the solution was then boiled to eliminate excess ammonia. After cooling, concentrated acetic acid was added for ¼ of the total volume of the solution. After a few minutes, 1 g of KI was added, and the resulting solution was titrated with a standard solution of sodium thiosulfate 2.50 mg Cu/mL. Near the endpoint, 2 mL of starch solution was added, and the endpoint was reached when the black color of the solution disappeared. The total volume of sodium thiosulfate used for the titration is proportional to the total Cu content of the solution (and, therefore, of the mineral). The measured Cu concentration in boleite was 13.9(2) wt%.

Gravimetric method for Pb concentration as lead molybdate. About 50 g of the "Solution A" was placed in a 200 mL beaker, and 2 g of ammonium chloride + 2 g of ammonium acetate were added. Lead was precipitated by adding (dropwise) 40 mL of an ammonium molybdate solution (4 g/L of ammonium molybdate + 10 mL of acetic acid). The solution was then heated to boiling for 2–3 min, allowing the suspension to settle. After a few minutes, a white precipitate was collected on a pre-weighed 30 mL porcelain filtering crucible (m_1) (porosity no. 4) and washed a few times with 5 mL of hot water containing 2% of ammonium nitrate. The porcelain crucible was then heated at 700 °C in a muffle furnace until a constant weight was reached (m_2). From the difference of weight (m_2–m_1), it is possible to calculate the total Pb concentration in boleite, precipitated as $PbMoO_4$, determined here to be 49.4(4) wt%.

Determination of Cu and Pb concentration by EDTA titration. About 10 g of the "Solution A" was placed in a 200 mL beaker; ammonium hydroxide was added until a white precipitate formed, and a few grains of murexide (as an indicator) were then added. The solution was titrated with a standard solution of EDTA 0.01 M. The endpoint was reached when the solution turned from yellow to violet. As the total volume of EDTA used is proportional to the total Cu+Pb content of the solution (and, therefore, of the mineral), the weight fraction of Cu and Pb in boleite can be calculated as: 1) Cu+Pb wt% = 13.90 (fixed) + 43.35 wt%, and Cu+Pb wt% = 13.89 + 49.40 (fixed) wt% [estimated standard deviation (e.s.d.) not determined].

Determination of F by ion selective electrode

A mass of 20 mg of boleite powder was placed in a 50 mL plastic test tube; then, 15 mL of water and 0.5 mL of nitric acid 1 M were added. A total of 2–3 mL of Total Ionic Strength Adjustment Buffer (commercial solution TISAB III) was added to the clear solution, along with 20 mL of water. The fluorine concentration was measured using a fluoride-selective electrode, following the standard addition method and using a certified reference solution of fluorine from 0.1 to 5 mg/L. The experimental findings proved that the F concentration in boleite was <0.01 wt% (e.s.d. not determined).

Loss-on-drying (moisture content) by heating

A mass of 100 mg of boleite powder was placed in a quartz crucible with a lid and heated in an oven from ambient temperature up to 105 °C (heating rate: 10 °C/min). The mass variation proved that the adsorbed H_2O content in boleite was <0.05 wt% (e.s.d. not determined).

Determination of CHN concentration

Analysis of total CHN showed that carbon and nitrogen were not detectable. Total hydrogen fraction was found to be 0.5(1) wt%.

Determination of minor elements concentration by ICP-OES and ICP-MS

All measurements (excluding Cs) were performed by both ICP-OES and ICP-MS. Cs concentration was measured by ICP-MS only.

Common and rare earth elements. A mass of 5–50 mg of boleite powder was placed in a 50 mL plastic test tube, and 2 mL of concentrated nitric acid solution was added. The resulting solutions were diluted with water and then filtered with 0.45 μm PTFE filters. A calibration protocol was applied with a blank solution and a series of ad hoc solutions (prepared using certified reference solutions and multi-elemental standard mix for ICP), with concentrations from 0.0001 to 0.01 mg/L for each element in ICP-MS, and from 0.01 to 1 mg/L in ICP-OES. The concentrations of the following elements were measured: Li, Na, K, Rb, Be, Mg, Sr, Ba, Ti, Zr, V, Cr, Mo, Mn, Fe, Co, Ni, Zn, Cd, Al, Tl, Si, P, As, Sb, Bi, B, Cs, Sn, Se, Nb, W, Se, Hf, Hg, Ga, Ge, In, Ta, Sc, Y, La, Ce, Pr, Nd, Sm, Eu, Gd, Tb, Dy, Ho, Er, Tm, Yb, Lu, U, and Th. Results and instrumental parameters are listed in Table 1.

Precious metals. A mass of 5–50 mg of boleite powder was placed in a 50 mL plastic test tube, and 5 mL of concentrated hydrochloric acid was added. The solutions were then diluted with water and filtered with 0.45 μm PTFE filters. In addition, a calibration protocol was applied with a blank solution and a series of ad hoc solutions (prepared using certified reference solutions and multi-elemental standard mix for ICP), with concentrations from 0.0001 to 0.01 mg/L in ICP-MS, and from 0.01 to 1 mg/L in ICP-OES for each of the following elements: Ru, Rh, Pd, Pt, Au, Os, Ir. Results are given in Table 1.

The concentrations of the major and minor elements in boleite, obtained by our multi-methodological approach, and the resulting chemical formula are given in Table 2.

Single-crystal X-ray and neutron diffraction

X-ray and neutron data collection and analyses

Two high-quality crystals, with different shapes and sizes, were selected for single-crystal X-ray and neutron diffraction experiments. Their quality was preliminarily assessed using a KUMA-KM4 four-circle X-ray diffractometer (COSPECT facility, University of Milan).

A prismatic pseudo-cubic crystal (ca. $0.120 \times 0.110 \times 0.105$ mm^3) of boleite was selected for X-ray intensity data collection at room temperature [293(1) K]. The data collection was performed with a Rigaku XtaLABSynergy-i X-ray diffractometer, equipped with a PhotonJet-i Mo*K*α microfocus source and a HyPix-6000HE HPC detector, at the Earth Sciences Department, University of Milan. Data were collected using an ad hoc routine (optimized by the CrysAlisPro suite; Rigaku-Oxford Diffraction

Table 1. Concentration of minor elements in boleite, as obtained by ICP-OES and ICP-MS (see text for details)

	%m/m	ICP-AES (nm)
K	0.14	766.490
Rb	0.06	780.023
Cs	0.04	(by ICP-MS)
Na	0.02	589.592
Ca	0.06	317.933
Cd	0.04	228.802
Tl	0.004	190.801

Note: The measured concentrations of Li, Be, Mg, Sr, Ba, Zr, V, Cr, Mo, Mn, Fe, Co, Ni, Zn, Al, Si, P, As, Sb, Bi, B, Sn, Se, Nb, W, Se, Hf, Hg, Ga, Ge, In, Ta, Sc, Y, La, Ce, Pr, Nd, Sm, Eu, Gd, Tb, Dy, Ho, Er, Tm, Yb, Lu, U, Th, Ru, Rh, Pd, Pt, Au, Os, and Ir are all <0.001%m/m.

Table 2. Concentration of the (significant) elements in boleite, as obtained by the multi-methodological approach of this study, and the resulting chemical formula

	%m/m	2σ
Pb	49.40	±0.40
Cu	13.90	±0.20
Ag	8.80	±0.20
Cl	20.00	±0.20
K	0.14	±0.03
Ca	0.06	±0.02
Cs	0.04	±0.02
Rb	0.06	±0.02
Cd	0.04	±0.02
Na	0.02	±0.01
Tl	0.004	n.d.
H	0.50	±0.10
OH	7.50[a]	

Notes: Empirical formula: $(K_{0.390}Ca_{0.165}Na_{0.095}Rb_{0.075}Cd_{0.040}Cs_{0.035}Tl_{0.002})_{\Sigma 0.80}Pb_{26.05}Ag_{8.93}Cu_{23.91}Cl_{61.64}(OH)_{48.39}$.
Simplified formula: $(K,Ca,Na,Rb,Cd,Cs)Pb_{26}Ag_9Cu_{24}Cl_{62}(OH)_{48}$.
[a] by difference.

2019) aimed to maximize the reciprocal space coverage and the quality of the intensity data, and based on an ω-scan strategy, with a 0.5° step size and an exposure time of 1 s/frame. A total number of 14 060 reflections were collected up to $2\theta_{max}$ of 69.3° (with d_{min} ~0.38 Å and $-13 \le h \le +22$, $-23 \le k \le +13$, and $-23 \le l \le +11$). The data reduction provided a metrically cubic unit cell, with $a = 15.2870(8)$ Å and $V = 3572.5(6)$ Å^3; 1152 reflections were found to be unique for symmetry ($R_{int} = 0.0442$, Laue class $m3m$) and 1092 with $Fo > 4\sigma(Fo)$. The reflection conditions were consistent with the space group $Pm\bar{3}m$. Intensity data were then integrated and corrected for the effects of Lorentz-polarization and of X-ray absorption using the ABSPACK routine (with a semi-empirical strategy), implemented in the CrysAlisPro package (Rigaku-Oxford Diffraction 2019). The final list of the intensity data was processed with the E-STATISTICS program [implemented in the WinGX package (Farrugia 1999)], and the Wilson plot and the statistics of distributions of the normalized structure factors suggested that the structure of boleite is centrosymmetric at >61% likelihood. Additional details are given in Online Materials[1] Table S1 and the CIF (Online Materials[1]).

A second crystal of boleite, with size 3.6 × 3.1 × 2.4 mm^3, was mounted on an Al pin and placed on a close-circuit displex device on the monochromatic four-circle D9 diffractometer at the Institute Laue-Langevin (ILL, Grenoble, France). Low-temperature neutron diffraction data were collected at 20(1) K (Archer and Lehmann 1986). The diffraction experiment was conducted using a wavelength of 0.8351 Å, as obtained from a Cu(220) monochromator, and a small two-dimensional area detector. An ad hoc data collection strategy was applied, based on a series of ω-scans (for low-Q reflections) and ω-2θ scans (for high-Q reflections), varying the ω-range in response to the instrument resolution curve. A total number of 3574 reflections was collected up to $2\theta_{max}$ of 103.9° (with d_{min} ~0.43 Å and $-20 \le h \le +20$, $-19 \le k \le +20$, and $-20 \le l \le +2$), of which 1573 reflections were unique for symmetry ($R_{int} = 0.0612$, Laue class $m3m$) and 1268 with $F_o > 4\sigma(F_o)$. Intensity data were integrated and corrected for background and Lorentz effects, using the Racer program (Wilkinson et al. 1988). Absorption correction was then applied, based on the shape of the crystal and its chemical composition, using the ILL program Datap (available in the online SXtalSoft repository, https://code.ill.fr/scientific-software/sxtalsoft). A metrically cubic unit cell was found, with $a = 15.148(1)$ Å and $V = 3475.9(7)$ Å^3, and reflection conditions were consistent with the space group $Pm\bar{3}m$, according to previous findings based on the X-ray data. The Wilson plot and the statistics of distributions of the normalized structure factors showed that the structure is centrosymmetric at ~86.5% likelihood. Further details pertaining to neutron data collection are given in Online Materials[1] Table S1 and the CIF (Online Materials[1]).

X-ray and neutron structure refinements

The X-ray structure refinement, based on the intensity data collected at room temperature (293 K), was performed using the SHELXL-2018/3 software (Sheldrick 2015) in the space group $Pm\bar{3}m$, starting from the structure model of Cooper and Hawthorne (2000), without any H site. X-ray atomic form factors for K, Pb, Ag, Cu, Cl, O, and H were taken from the *International Tables for Crystallography Vol. C*. Secondary isotropic extinction effect was corrected according to Larson's formalism (1967), implemented in SHELX; however, the correction was found to be insignificant. The *K* site was first modeled as fully occupied by potassium, leaving the occupancy factor to vary. After the first cycles of isotropic refinement, convergence was rapidly achieved. The next cycles of refinement were then conducted with the atomic sites modeled anisotropically, until convergence was achieved. The two independent H sites, i.e., *H*1 and *H*2 (Online Materials[1] Table S2), were then added; their atomic coordinates were taken from the neutron structure refinement (see below) and modeled as isotropic (restraining the two sites to share the same isotropic displacement parameter). With this structural model, convergence was achieved, and the variance-covariance matrix reported no significant correlation among the refined parameters. Additionally, all principal mean-square atomic displacement parameters were positive. The most significant residual peak, found in the difference-Fourier map of the electron density function, lies at ~0.7 Å from the *Pb*3 (i.e., +2.0 *e*–/Å^3). The final $R_1(F)$ was 0.0385, for 1092obs./62par. Additional details of the X-ray structure refinement are listed in Online Materials[1] Table S1; the atomic site coordinates and displacement parameters (including the principal root-mean-square components) are given in Online Materials[1] Tables S2, S3, and S4 and the CIF (Online Materials[1]). Some selected interatomic distances and angles are listed in Table 3.

The neutron structure refinement, based on the intensity data collected at 20 K, was also performed using the SHELXL-2018/3 software (Sheldrick 2015) in the space group $Pm\bar{3}m$, starting from the H-free structure model of Cooper and Hawthorne (2000). Neutron scattering lengths of K, Pb, Ag, Cu, Cl, O, and H were taken from Sears (1986). Secondary isotropic extinction effect was corrected according to the formalism of Larson (1967), implemented in SHELX, but the correction was found to be insignificant [i.e., EXTI: 0.00024(10)]. The *K* site was modeled as fully occupied by potassium, leaving its occupancy factor to vary led to fluctuating refined values. After the first cycles of isotropic refinement, convergence was rapidly achieved with two significant minima in the difference-Fourier map of the nuclear density function, at a distance from *O*1 and *O*2 sites compatible with O-H

Table 3. Relevant bond distances (Å) and angles (°) based on the neutron structure refinement (at 20 K) and the X-ray refinement (at 293 K) of boleite

	Neutron	X-ray
K-*Cl*5 (×12)	3.630(2)	3.694(4)
*Pb*1-*Cl*2 (×4)	2.946(2)	2.971(2)
*Pb*1-*Cl*5 (×4)	3.003(1)	3.046(1)
*Pb*2-*O*2 (×3)	2.462(2)	2.477(5)
*Pb*2-*Cl*2 (×3)	3.272(2)	3.299(1)
*Pb*2-*Cl*5 (×3)	3.030(1)	3.0666(8)
*Pb*3-*O*1 (×2)	2.733(2)	2.787(1)
*Pb*3-*Cl*4 (×2)	2.941(1)	2.9595(4)
*Pb*3-*Cl*2 (×4)	3.032(1)	3.066(1)
*Ag*1-*Cl*3	2.625(4)	2.630(4)
*Ag*1-*Cl*1 (×4)	2.667(1)	2.692(2)
*Ag*2-*Cl*3 (×2)	2.601(2)	2.608(4)
*Ag*2-*Cl*4 (×4)	2.807(2)	2.843(3)
Cu-*O*2 (×2)	1.949(1)	1.960(2)
Cu-*O*1 (×2)	1.953(1)	1.959(3)
Cu-*Cl*1	2.901(1)	2.921(2)
Cu-*Cl*2	2.783(1)	2.822(2)
*O*1-*H*1	0.979(4)	0.98(6)
*O*1-*H*1[a]	0.999	1.04
*O*1 . . . *Cl*3	3.193(2)	3.212(5)
*H*1 . . . *Cl*3	2.216(4)	2.25(5)
*O*1-*H*1 . . . *Cl*3	175.3(4)	169(4)
*O*2-*H*2	0.978(4)	0.92(8)
*O*2-*H*2[a]	0.997	0.95
*O*2 . . . *Cl*4	3.101(2)	3.133(5)
*H*2 . . . *Cl*4	2.123(4)	2.21(8)
*O*2-*H*2 . . . *Cl*4	179.1(3)	177(6)

[a] Bond distance corrected for "riding motion" effect, following Busing and Levy (1964).

groups. Two independent H sites, i.e., *H*1 and *H*2 (Online Materials[1] Table S2), which were then added (as H has a negative neutron scattering length), were first modeled as isotropic. The next cycles of refinement were conducted with all the atomic sites modeled anisotropically (H sites included), until convergence was achieved. At the end of refinement, no significant correlation among the refined variables was observed in the variance-covariance matrix, and all the principal mean-square atomic displacement parameters were positive. The final min/max residuals were –3.4 fm/Å^3 (at ~0.3 Å from the *K* site) and +3.8 fm/Å^3 (at ~0.9 Å from the *K* site), confirming a positional disorder around the center of inertia of the large 18-node cage, where the *K* site is nominally located at ½, ½, ½. The final $R_1(F)$ was 0.0695, for 1268obs./68par. Additional details pertaining to the neutron structure refinement are listed in Online Materials[1] Table S1; the atomic site coordinates and displacement parameters are given in Online Materials[1] Tables S2, S3, and S4, and the CIF (Online Materials[1]), and some selected interatomic distances and angles are listed in Table 3.

Discussion and Implications

The chemical and crystallographic data of boleite from the Amelia Mine (Boléo District), obtained in this study by a multi-methodological approach, fully confirm the general structural model of this mineral previously reported in the literature (Rouse 1973; Cooper and Hawthorne 2000), but only partially support its general chemical formula [i.e., $KPb_{26}Ag_9Cu_{24}Cl_{62}(OH)_{48}$].

Although elemental populations at the *Pb*1, *Pb*2, *Pb*3, *Ag*1, *Ag*2, and *Cu*-sites (Online Materials[1] Table S2) are basically confirmed, and represented by Pb, Ag, and Cu, respectively, this is not the case for the *K* site. A series of significant substituents is detected at the *K* site, which is not only populated by K, but also by Ca, Na, Rb, Cd, and Cs (with Ca > Na > Rb > Cd > Cs in atoms per formula unit). The obtained empirical chemical formula is: $(K_{0.390}Ca_{0.165}Na_{0.095}Rb_{0.075}Cd_{0.040}Cs_{0.035}Tl_{0.002})_{\Sigma 0.80}Pb_{26.05}Ag_{8.93}Cu_{23.91}Cl_{61.64}(OH)_{48.39}$, of which the simplified formula should be given as: $(K,Ca,Na,Rb,Cd,Cs)Pb_{26}Ag_9Cu_{24}Cl_{62}(OH)_{48}$ (Table 2). Cd could also be considered as a potential substituent of Ag or Cu, and therefore the simplified formula transforms to $(K,Ca,Na,Rb,Cs)Pb_{26}Ag_9Cu_{24}Cl_{62}(OH)_{48}$. Based on our empirical formula, the expected charge contribution provided by the *K* site, with its multi-elemental population, is close to the ideal one, being +1.007 (including Cd) or +0.927 (excluding Cd). Accordingly, neutron (at 20 K) and X-ray (at 293 K) structural models consistently show that substitutional disorder affects the *K* site. Such a (static) disorder is manifested by a large and unusual displacement parameter (forced to have a spherical shape by symmetry), due to differences in the local bonding topology among K, Ca, Na, Rb, (Cd), and Cs, statistically populating the same site. In fact, it is very unlikely that elements such as Ca or Na (or Cd) can have a bonding configuration with coordination number CN = 12 and bond distances of ca. 3.69 Å at 293 K (or ca. 3.63 Å at 20 K, Table 3). We can then presume that some of the aforementioned elements are variably displaced from the center of inertia of the large 18-node cage, at ½, ½, ½. Consistently, the effect of disorder at the *K* site is significant even at 20 K (neutron data, Online Materials[1] Tables S2, S3, and S4), leading us to exclude dynamic effects. A side effect of substitutional disorder at the *K* site is even reflected by the ellipticity ratio of the displacement ellipsoid of the *Cl*5 site, which forms the coordination net of the *K* site (i.e., *K*-*Cl*5 × 12, Table 3): the ratio (defined considering the longest and the shortest principal root-mean-square components, RMS_{max}/RMS_{min}) is the highest among all the atomic site of the boleite structure, at both 293 and at 20 K (Online Materials[1] Tables S3 and S4). However, the disorder at the *K* site does not generate any significant effect at the lattice level, as proved by the fully indexed neutron and X-ray diffraction patterns (with a cubic unit cell with edge of ca. 15.29 Å at room conditions).

The other building units of the boleite structure, as previously described by Cooper and Hawthorne (2000), are here confirmed, in shape and composition:

- one chain system, made by cages consisting of six $AgCl_5$ groups that form square pyramids [whose square faces describe a cube centered at (0,0,0)] connected by $AgCl_6$-octahedra and running along the three principal crystallographic directions (Fig. 1a);
- a second chain system consisting of large cages made by the interconnection of [6Pb+12Cl] sites (with 18 nodes), connected by smaller [6Pb+8Cl] cages (with 14 nodes) and running along the three principal crystallographic directions (Fig. 1b);
- clusters made by three face-sharing distorted CuO_4Cl_2 octahedra (Fig. 1d) connected to form 8-membered rings perpendicular to each of the fourfold axis.

The combination of these building units results in the complex structural "framework" of boleite (Fig. 1c), containing the aforementioned small and large cages.

Chemical data obtained in this study show no significant evidence of potential substituents of Pb, Ag, and Cu (Tables 1 and 2).

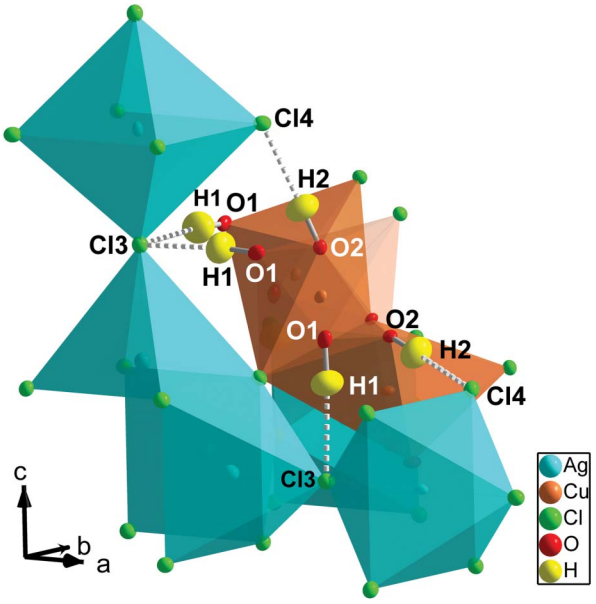

Figure 2. The H-bonding network into the crystal structure of boleite, based on the single-crystal neutron structure refinement of this study (data collected at 20 K). Details pertaining to H bond distances and angles are listed in Table 3. Polyhedral configuration is shown in Figures 1a–1d. Displacement ellipsoid probability factor: 90%. (Color online.)

Notably, the concentration of REE, PGE, and other industrially relevant elements is insignificant (Tables 1 and 2). Despite a lack of crystallographic evidence, chemical data suggest that partial Cl^- vs. OH^- substitution can also occur. Other potential substituents of Cl^-, such as F^-, have not been detected at a significant level.

The neutron structure refinement allowed a reliable location of the two independent H sites (i.e., *H*1 and *H*2, Online Materials[1] Table S2), both belonging to hydroxyl groups (i.e., *O*1-*H*1 and *O*2-*H*2, Table 3), and a realistic model of their libration regime: both the *H*-sites show principal root-mean-square components that are 2–3 times those of the O sites, and ellipticity ratios lower than 1.43. The occurrence of molecular H_2O in the structure of boleite can be unambiguously ruled out, in contrast to what was reported by Abdul-Samad et al. (1981), and in accordance with the experimental findings of Cooper and Hawthorne (2000) and Frost et al. (2003). The H-bonding network in the structure of boleite can be reliably described on the basis of the neutron structural model, with two energetically favorable bonds (Fig. 2):

(1) one with *O*1 as a donor and *Cl*3 as an acceptor, with *O*1-*H*1 of ~0.999 Å (as corrected by riding-motion effect), *O*1···*Cl*3 = 3.193(2) Å, *H*1···*Cl*3 = 2.216(4) Å, and *O*1-*H*1···*Cl*3 = 175.3(4)° (Table 3); and

(2) the other with *O*2 as a donor and *Cl*4 as an acceptor, with *O*2-*H*2 of ~0.997 Å (corrected by riding-motion effect), *O*2···*Cl*4 = 3.101(2) Å, *H*2···*Cl*4 = 2.123(4) Å, and *O*2-*H*2···*Cl*4 = 179.1(3)° (Table 3).

The bonding schemes show that both configurations reflect moderate H-mediated interactions, with almost ideal linear O_{donor}-H···$Cl_{acceptor}$ geometry. Other potential acceptors [e.g., *O*1, with *O*2-*H*···*O*1 = 89.6(2)° and *O*2···*O*1 = 2.893(1) Å], implying a bifurcated bonding scheme, can be ruled out, as they would be energetically unfavorable. However, the bonding configuration of the acceptor atoms is different: *Cl*3 belongs to the coordination net of *Ag*1 and *Ag*2, whereas *Cl*4 is shared by *Ag*1, *Ag*2, and *Pb*3 (Table 3). In some way, this also influences the shape of the displacement ellipsoids, such that the RMS_{max}/ RMS_{min} ratio is higher for *Cl*4 (at 293 and 20 K, Online Materials[1] Table S4). The powder IR absorption spectrum for boleite pertaining to the O-H stretching region, reported by Cooper and Hawthorne (2000), shows a sharp band at ~3388 cm^{-1}. The Raman spectrum of a boleite crystal, reported by Frost et al. (2003), shows three broad bands at 3448, 3408, and 3371 cm^{-1}, interpreted as the antisymmetric (i.e., 3448 and 3408 cm^{-1}) and symmetric (i.e., 3371 cm^{-1}) stretching vibrations of the O-H groups. The latter finding better reflects the scenario based on the neutron structural model presented in this study: the independent H-bonds in the boleite structure are similar, but not identical; therefore, more than one signature is expected for each vibrational mode. However, similar vibrational energies often lead to a convolution of signals, resulting in broad bands in vibrational spectra. The Raman spectrum reported (and interpreted) by Frost et al. (2003) range between 100 and 4000 cm^{-1}: in the low-wavenumber region (from 100 to 1000 cm^{-1}), the authors identified two types of bands ascribed to the hydroxyl deformation modes and to Pb-Cl and Cu-Cl vibrations, according to the general structural model of boleite reported by Cooper and Hawthorne (2000) and in this study.

The effects of temperature on the crystal structure of boleite are modest, as can be deduced by the unit-cell parameters and the structural models based on the X-ray refinement (data collected at 293 K) and on the neutron refinement (data collected at 20 K). In response to the low temperature, the unit-cell volume decreases by 2.70(4)%, so that the volume thermal expansion coefficient (valid between 20 and 293 K) is: $\alpha_V = 9.9(2)\cdot10^{-5}$ K^{-1}. At the atomic scale, the interatomic bond distances experience a general low temperature-induced reduction of the bond lengths, ranging from ~0.06 Å (e.g., *K*-*Cl*5, Table 3) to ~0.01 Å (e.g., *Ag*2-*Cl*3, Table 3); the average contraction is ~0.02–0.03 Å, modest but significant. The atomic displacement factors, represented by U_{eq} ($Å^2$), show a more pronounced variation in response to temperature: the values refined at 293 K are, on average, 3–4 times higher than those at 20 K, but scattered over a wide range (from ~2.5 to ~10 times, Online Materials[1] Table S2).

Structural data, particularly at low temperatures, and chemical data obtained in this study may support investigation of novel boleite-type materials in searching for mesoscopic spin systems; the combination of mesoscopic system size and strong quantum effects represents a new front of applications in quantum simulation, information storage, and processing in quantum computers. In this respect, a recent study by Dreier et al. (2018), based on magnetic susceptibility measurements (2–300 K) and exact diagonalization calculations, showed that the boleite structure is an interesting example of a highly frustrated mesoscopic quantum spin system, whose isolated 24-spin cluster spin systems can be measured experimentally, or even modeled using a simple numerically accessible Hamiltonian.

The protocol used in this study for the chemical analyses, to circumvent issues with EPMA-WDS analysis, proved to be appropriate for such a chemically complex material. The lack of full-chemical characterization of boleite during the past decades may be due to similar issues with EPMA-WDS analysis, likely caused by material degradation under the electron beam (with consequent dehydration and element migration) and/or by difficulties in appropriately modeling matrix effects. The multi-methodological approach we used for chemical characterization of boleite has been successfully applied to other hydrous minerals, including those containing light elements as principal constituents, e.g., Li, Be, B, and N (e.g., Gatta et al. 2014, 2019, 2020, 2022, 2023; Lotti et al. 2018), and we expect it can be used more widely when conventional protocols, based on electron beam techniques, prove inadequate.

Acknowledgments and Funding

The authors thank the Institut Laue-Langevin (Grenoble, France) for the allocation of the neutron beamtime (DOI: 10.5291/ILL-DATA.5-11-452). X-ray (with KUMA diffract.) and EPMA-WDS data were collected using the facilities of the UniTech COSPECT – University of Milan (Italy). G.D.G., T.B., and M.M. acknowledge the support of the Italian Ministry of Education (MUR) through the projects "Dipartimenti di Eccellenza 2023–2027." The Associate Editor, Oliver Tschauner, and an anonymous reviewer are warmly thanked for the revision of the manuscript.

References Cited

Abdul-Samad, F.A., Alun Humphries, D., Thomas, J.H., and Williams, P.A. (1981) Chemical studies on the stabilities of boleite and pseudoboleite. Mineralogical Magazine, 44, 101–104, https://doi.org/10.1180/minmag.1981.44.333.16.

Archer, J. and Lehmann, M.S. (1986) A simple adjustable mount for a two stage cryorefrigerator on an Eulerian cradle. Journal of Applied Crystallography, 19, 456–458, https://doi.org/10.1107/S0021889886088957.

Busing, W.R. and Levy, H.A. (1964) The effect of thermal motion on the estimation of bond lengths from diffraction measurements. Acta Crystallographica, 17, 142–146, https://doi.org/10.1107/S0365110X64000408.

Conly, A.G. (2003) Origin of the Boléo Cu-Co-Zn deposit, Baja California Sur, México: Implications for the interaction of magmatic-hydrothermal fluids in a low temperature hydrothermal system, 433 p. Ph.D. thesis, University of Toronto.

Cooper, M.A. and Hawthorne, F.C. (2000) Boleite: Resolution of the formula, $KPb_{26}Ag_9Cu_{24}Cl_{62}(OH)_{48}$. Canadian Mineralogist, 38, 801–808, https://doi.org/10.2113/gscanmin.38.4.801.

Del Rio Salas, R., Ruiz, J., Ochoa Landín, L., Noriega, O., Barra, F., Meza-Figueroa, D., and Paz Moreno, F. (2008) Geology, Geochemistry and Re-Os systematics of manganese deposits from the Santa Rosalía Basin and adjacent areas in Baja California Sur, México. Mineralium Deposita, 43, 467–482, https://doi.org/10.1007/s00126-008-0177-3.

Dreier, E.S., Holm, S.L., Lønbæk, K., Hansen, U.B., Medarde, M., Živković, I., Babkevich, P., Ruminy, M., Casati, N., Piovano, A., and others. (2018) 24-spin clusters in the mineral boleite $KPb_{26}Ag_9Cu_{24}Cl_{62}(OH)_{48}$. Physical Review. B, 97, 014416, https://doi.org/10.1103/PhysRevB.97.014416.

Farrugia, L.J. (1999) WinGX suite for small-molecule single-crystal crystallography. Journal of Applied Crystallography, 32, 837–838, https://doi.org/10.1107/S0021889899006020.

Friedel, G. (1906) Contribution à l'étude de la boléite et de ses congénères. Bulletin de la Société Française de Minéralogie, 29, 14–55, https://doi.org/10.3406/bulmi.1906.2769.

Frost, R.L. and Williams, P.A. (2004) Raman spectroscopy of some basic chloride containing minerals of lead and copper. Spectrochimica Acta Part A: Molecular and Biomolecular Spectroscopy, 60, 2071–2077, https://doi.org/10.1016/j.saa.2003.11.007.

Frost, R.L., Williams, P.A., and Martens, W. (2003) Raman spectroscopy of the minerals boléite, cumengéite, diaboléte and phosgenite — Implications for the analysis of cosmetics of antiquity. Mineralogical Magazine, 67, 103–111, https://doi.org/10.1180/0026461036710088.

Gatta, G.D., Nénert, G., Guastella, G., Lotti, P., Guastoni, A., and Rizzato, S. (2014) A single-crystal neutron and X-ray diffraction study of a Li,Be-bearing brittle mica. Mineralogical Magazine, 78, 55–72, https://doi.org/10.1180/minmag.2014.078.1.05.

Gatta, G.D., Guastoni, A., Lotti, P., Guastella, G., Fabelo, O., and Fernandez-Diaz, M.T. (2019) A multi-methodological study of kurnakovite: A potential B-rich aggregate. American Mineralogist, 104, 1315–1322, https://doi.org/10.2138/am-2019-7072.

——— (2020) A multi-methodological study of kernite, a mineral commodity of boron. American Mineralogist, 105, 1424–1431, https://doi.org/10.2138/am-2020-7433.

Gatta, G.D., Guastella, G., Capelli, S., Comboni, D., and Guastoni, A. (2022) On the crystal-chemistry of meyerhofferite, $CaB_3O_6(OH)_5{\cdot}H_2O$. Physics and Chemistry of Minerals, 49, 22, https://doi.org/10.1007/s00269-022-01199-1.

Gatta, G.D., Guastella, G., Guastoni, A., Gagliardi, V., Cañadillas-Delgado, L., and Fernandez-Diaz, M.T. (2023) A neutron diffraction study of boussingaultite, $(NH_4)_2[Mg(H_2O)_6](SO_4)_2$. American Mineralogist, 108, 354–361, https://doi.org/10.2138/am-2022-8385.

Gossner, B. (1928) The crystal form of boléite. American Mineralogist, 13, 580–582.

Hocart-Strasbourg, R. (1930) II. Sur la détermination des paramètres de la boléite, de la pseudoboléite et de la cumengéite, au moyen des rayons X. Zeitschrift für Kristallographie. Crystalline Materials, 74, 20–24, https://doi.org/10.1524/zkri.1930.74.1.20.

Larson, A.C. (1967) Inclusion of secondary extinction in least-squares calculations. Acta Crystallographica, 23, 664–665, https://doi.org/10.1107/S0365110X67003366.

Lotti, P., Gatta, G.D., Demitri, N., Guastella, G., Rizzato, S., Ortenzi, M.A., Magrini, F., Comboni, D., Guastoni, A., and Fernandez-Diaz, M.T. (2018) Crystal-chemistry and temperature behavior of the natural hydrous borate colemanite, a mineral commodity of boron. Physics and Chemistry of Minerals, 45, 405–422, https://doi.org/10.1007/s00269-017-0929-7.

Mallard, E. and Cumenge, É. (1891) Sur une nouvelle espèce minérale, la Boléite. Bulletin de la Société Française de Minéralogie, 14, 283–293, https://doi.org/10.3406/bulmi.1891.2244.

Rigaku Oxford Diffraction. (2019) CrysAlisPro Software system, version 1.171.40.67a. Rigaku Corporation.

Rouse, R.C. (1973) The crystal structure of boleite—A mineral containing silver atom clusters. Journal of Solid State Chemistry, 6, 86–92, https://doi.org/10.1016/0022-4596(73)90208-9.

Sears, V.F. (1986) Neutron Scattering Lengths and Cross-Sections. In K. Sköld and D.L. Price, Eds., Neutron Scattering, Methods of Experimental Physics, Vol. 23A, 521–550. Academic Press.

Sheldrick, G.M. (2015) Crystal structure refinement with SHELXL. Acta Crystallographica Section C: Structural Chemistry, 71, 3–8, https://doi.org/10.1107/S2053229614024218.

Wilkinson, C., Khamis, H.W., Stansfield, R.F.D., and McIntyre, G.J. (1988) Integration of single-crystal reflections using area multidetectors. Journal of Applied Crystallography, 21, 471–478, https://doi.org/10.1107/S0021889888005400.

Wilson, I.F. and Rocha, V.S. (1955) Geology and mineral deposits of the Boleo copper district, Baja California, Mexico. U.S. Geological Survey Professional Paper #273, 134 p. US Government Printing Office.

Manuscript received December 14, 2024
Manuscript accepted February 23, 2025
Accepted manuscript online March 6, 2025
Manuscript Handled by Oliver Tschauner

Endnotes:

[1]Deposit item AM-25-109721. Online Materials are free to all readers. Go online, via the table of contents or article view, and find the tab or link for supplemental materials. The CIF has been peer-reviewed by our Technical Editors.